

Clean, Robust Alkali Sources by Intercalation within Highly-Oriented Pyrolytic Graphite

Rudolph N. Kohn, Jr.,^{1, a)} Matthew S. Bigelow,² Mary Spanjers,³ Benjamin K. Stuhl,¹ Brian L. Kasch,³ Spencer E. Olson,³ Eric A. Imhof,¹ David A. Hostutler,³ and Matthew B. Squires³

¹⁾*Space Dynamics Laboratory, Albuquerque, New Mexico 87106, USA*

²⁾*Applied Technology Associates, Albuquerque, New Mexico 87123, USA*

³⁾*Air Force Research Laboratory, Kirtland AFB, New Mexico 87117, USA*

We report the fabrication, characterization, and use of rubidium vapor dispensers based on highly-oriented pyrolytic graphite (HOPG) intercalated with metallic rubidium. Compared to commercial chromate salt dispensers, these intercalated HOPG (IHOPG) dispensers hold an order of magnitude more rubidium in a similar volume, require less than one-fourth the heating power, and emit less than one-half as many impurities. Appropriate processing permits exposure of the IHOPG to atmosphere for over ninety minutes without any adverse effects. Intercalation of cesium, potassium, and lithium into HOPG have also been demonstrated in the literature, which suggests that IHOPG dispensers may also be made for those metals.

^{a)}Electronic mail: rudy.kohn@sdl.usu.edu

I. INTRODUCTION

Alkali metals serve as the atomic backbone for a wide variety of physics experiments. Alkalis' simple electronic structure and strong transitions facilitate laser cooling and make them very attractive candidates for atomic sensors. In experiments using alkali metals, the on-demand production of a clean, dilute vapor is often the first crucial step. The stringent requirements of modern cold atom experiments mean that significant improvements in this first step can positively impact the rest of the experiment. This work introduces a new architecture for producing extremely pure alkali vapors using intercalated graphite, and compares this new architecture to commercially available dispensers.

Many methods exist to produce pure, dilute atomic vapors. However, experimental parameters often limit which methods are viable. For example, an atomic beam experiment might need a source with high flux and directionality, but stationary or slow-moving cold atom experiments often depend upon extremely pure, dilute vapors, so that the atoms can be trapped and cooled with minimal interference from background gas. The desired background pressures are often orders of magnitude below the room temperature vapor pressures of the metals, impeding the use of pure metallic sources. Other characteristics, such as capacity, activation temperature, ease of handling, and total vapor produced frequently place other restrictions on the source.

For the production of pure, dilute alkali vapors, there are two general architectures in common use. The first uses ovens, usually emitting effusive beams, which offer high purity and capacity (grams) and low activation temperature (~ 100 °C for rubidium). However, simple ovens produce enough vapor to have deleterious effects on pumps and vacuum quality.¹ Negative effects on vacuum can be mitigated, but generally at the expense of increased complexity. The large quantities of pure alkali used can present difficulties for safe handling and disposal, as well.²

The second general architecture uses chromate salts and non-evaporable getter (NEG) material to produce a reasonably pure alkali vapor.^{3,4} Commercial chromate salt dispensers are compact and easy to handle, but they have relatively low capacity (~ 10 mg for a 30 mm long dispenser), much higher activation temperatures (~ 500 °C for rubidium chromate), and can emit significant quantities of unwanted gas under certain conditions. A typical chromate salt dispenser contains NEG material to inhibit the release of unwanted gases. However,

prolonged periods at room temperature can collect unwanted gases in the NEG material or on the nearby chamber walls, and improperly degassing before activation can contaminate the source.⁵ We have observed that extended periods at room temperature produce a measurable pressure spike when the chromate dispenser is next heated, which can be traced to either gas adsorbed onto the steel container of the dispenser or absorbed into its NEG material, or adsorbed onto chamber surfaces near the dispenser, which are heated during activation.

We present an alternative source of alkali vapor which compares favorably to the chromate salt architecture in size, ease of handling, and ease of activation while improving on the purity of their output and increasing their capacity to ~ 100 mg in a similar volume. Highly-oriented pyrolytic graphite (HOPG), essentially graphite with a high degree of internal order, can absorb relatively large amounts of foreign chemicals between its graphene-like layers. This behavior, known as intercalation, has been studied since at least the 1940s.^{6,7} Graphite and HOPG have frequently been used as getters for alkali vapors because of this behavior.^{8,9} The characteristics of intercalated HOPG (IHOPG) as a dispenser have been examined in the context of vapor deposition,¹⁰ but, to the best of our knowledge, no examination of its compatibility with ultra-high vacuum (UHV) or modern cold-atom experiments has been made. Many materials are known to intercalate into HOPG, but of special interest here are the four alkalis known to intercalate relatively easily: lithium, potassium, rubidium, and cesium.^{11–16} Studies have shown that sodium is much more difficult to intercalate into graphite,¹⁷ therefore it seems unlikely that reliable dispensers can be made for sodium. Although examples of cesium, potassium, and lithium intercalation are present in the literature, the work described here uses rubidium exclusively. We devised a method to reliably intercalate HOPG with rubidium, make the IHOPG relatively stable in atmosphere, and controllably dispense rubidium vapor under vacuum.

We describe the methods for producing rubidium IHOPGs in Section II. The apparatus used to compare the dispensers is detailed in Section III, and then, two comparisons are made. The first, in Section IV, compares the purity of the output vapor of both dispensers in a steady-state configuration. The second, in Section V, compares the undesired gas which accumulates on, in, or near the dispensers after extended periods at room temperature. In both cases, the IHOPG dispenser produced less undesired gas than the chromate dispenser. In general, heating dispensers emits waste gases, either from the dispenser itself or from gases adsorbed onto nearby walls. Emitted rubidium interacts with background gas, caus-

ing a getter effect. Over the range of rubidium emission rates we tested, the waste gases produced by heating the chromate dispenser consistently overwhelmed this getter effect. However, at sufficiently high rubidium output rates the waste gases produced by heating the IHOPG were so inconsequential that the pressure in the chamber actually decreased. Aside from the IHOPG dispenser used for these tests, another IHOPG dispenser has been successfully integrated into a cold atom experiment loading grating magneto-optical traps (MOTs).¹⁸ Another system in current daily use contains an IHOPG for dispensing rubidium, and regularly produces Bose-Einstein condensates.

II. FABRICATION AND OPERATION

Alkalis are intercalated into HOPG by placing a heated sample of HOPG in close proximity to vapor at high enough (\gtrsim mTorr) pressure. The heat allows alkali atoms to diffuse between its graphene-like layers. Specific temperatures are given for rubidium. Cesium has a very similar melting point and vapor pressure, so the temperatures required may also be very similar. Potassium and lithium, however, melt at much higher temperatures and have a much lower vapor pressure, so higher temperatures will almost certainly be required.

The procedure detailed below reliably produces rubidium IHOPG dispensers with about 1 mg of rubidium per mm³ of dispenser. The initial samples of HOPG were 7 x 7 x 1 mm, but successful intercalation increased their volume by a factor between 2 and 3. Several optional steps, detailed in Subsection II A, improve ease of handling.

The structure of the original HOPG affected how reliably they could be intercalated. HOPG is typically graded by crystallographic order, characterized by two parameters: mosaic angle and grain size. Mosaic angle is a measure of the dispersion of the angles of crystallites in the sample.¹⁹⁻²¹ The grain size is typically measured in microns or millimeters and describes how far apart, on average, grain boundaries can be found. In the early stages of our work, we experimented with samples with different levels of order and found that samples with higher crystallographic order loaded and dispensed more reliably. The dispensers described here were all produced from HOPG samples with mosaic angles of 0.8 ± 0.2 degrees, and with average grain sizes between 0.5 and 1.0 millimeters.

We prebake all of our HOPGs at 250 °C under high vacuum to eliminate surface impurities and degas the sample. 48-72 hours at this temperature, with a turbomolecular pump to

maintain vacuum, is sufficient to bake out a reasonably clean HOPG sample, removed from its packing material and handled with gloves. After the prebake, we remove the sample to a dry nitrogen atmosphere and add elemental rubidium into the chamber. The glove box we use for this purpose is fed dry nitrogen from a dewar source, but any inert gas (e.g. argon) would likely work just as well. In practice, we usually pour a few drops of molten rubidium onto the HOPG, but other delivery methods, such as small pieces of solid rubidium dropped into the chamber should work just as well, since the intercalation process is driven by heating the HOPG and exposing it to vapor,^{22,23} which will be present when the chamber is heated in either case. Before heating, we attach the chamber to an oil-free roughing pump, reducing the background pressure to the milliTorr range. The rough vacuum removes unwanted gases in the chamber, which can impair intercalation. We then seal off the chamber containing the HOPG and rubidium under rough vacuum and heat the chamber to 125-150 °C for at least 48 hours to intercalate.

After 48 hours, we turn off the heaters and remove the cooled chamber to a dry nitrogen atmosphere to examine the HOPG. Successfully intercalated HOPGs dramatically increase in thickness, with a 1 mm thick HOPG swelling to 2 or 3 mm after intercalation. This expansion is strong evidence that the process creates high stresses in the HOPG sample. We have observed samples that broke into several pieces during intercalation, and an attempt to load rubidium into graphene foam reduced the sample to dust. Based on these observations, we infer that larger grain size inhibits structural damage to the HOPG.

The structure and dimensions of IHOPG are fairly well known¹⁵. IHOPG has several different stable structures with different stoichiometric ratios. The structure with the most intercalated material has the formula XC_8 , corresponding to 0.89 g of rubidium for each gram of carbon. However, our loaded samples usually gain more mass than this, with a 110 mg HOPG gaining 100-220 mg of rubidium. The expansion in size is also larger than predicted by the expected structure: the known thickness difference between pure and maximally intercalated HOPG is 68%—much less than the 100-200% increases observed in our samples. In addition, IHOPGs exposed to air for long periods tend to expand further, with layers splitting apart as the rubidium oxidizes. These observations strongly suggest that additional rubidium is making its way between the layers of the HOPG, pushing them further apart and adding more rubidium to the dispensers than expected in a pure intercalation.

Once the HOPGs are loaded, they are placed in a vacuum chamber and heated in order

to liberate the intercalated rubidium. The IHOPGs begin emitting rubidium vapor when heated over some activation temperature, which varies somewhat from sample to sample. Typical activation temperatures range from 125-160 °C, and seems to roughly correlate with the amount of intercalated rubidium. Additional heating over the activation temperature increases the emission rate. Dispensers rapidly plate rubidium onto nearby glass at temperatures of 250 °C. A newly loaded dispenser held at 250 °C depleted itself in about 72 hours, implying a rate of 2-3 milligrams per hour at that temperature. A different IHOPG sample emitted no measurable rubidium over a 12 hour period at 150 °C, but at 170 °C, it produced enough rubidium to observe laser-induced fluorescence in a small chamber after about 10 minutes, suggesting an output rate of about 0.5 nanograms per hour, taking into account the laser power and the sensitivity of the infrared scope. Our attempts to measure rubidium vapor emitted from IHOPGs at room temperature under vacuum have all been below the detection limit.

We attempted to heat the IHOPGs above the activation temperature with several methods. Of these methods, we had success with two: conductive heating from outside the chamber and inductive heating across a glass wall. For conductive heating, a resistive tape outside the chamber heats the IHOPG through the chamber wall. This method allows easy monitoring of the IHOPG temperature with a thermocouple, which is useful for characterizing a sample's activation temperature. Conductive heating might also be accomplished by attaching the IHOPG to a heating element inside the chamber. For inductive heating, a wire coil outside the chamber, oriented in the same plane as the layers of the IHOPG and carrying a large, rapidly oscillating current, heats the sample by inducing eddy currents in the graphite. In a glass chamber, the IHOPG can be epoxied to a chamber wall or simply rest on the chamber bottom. The distance between the coil and the IHOPG controls the temperature and emission rate, though measuring the absolute temperature using this method is difficult.

A. Improving Ease of Handling

Although the dispenser can be used immediately after loading, it usually leaves the intercalation chamber coated in a layer of metallic rubidium. Failing to remove the surface rubidium results in rapid reactions with air and moisture upon exposure, and can cause

structural damage to the IHOPG after only a few minutes. A few optional steps greatly ease handling in atmosphere. First, we transfer the IHOPG into a clean glass vacuum chamber and heat it with a heater tape to between 100 and 120 °C, with a turbomolecular pump maintaining vacuum. We maintain the temperature below the activation temperature to remove surface rubidium without dispensing from between the layers. Depending on the amount of surface rubidium, this takes 24-48 hours. We gauge the depletion of surface rubidium by observing laser fluorescence on the D2 line at 780 nm. Heated surface rubidium produces enough vapor to observe laser-induced fluorescence when a near-resonant laser is passed through the chamber. When this fluorescence disappears, the surface rubidium has been depleted and it is safe to move on to the next step.

After removing the surface rubidium, we slowly raise the temperature of the IHOPG to find the activation temperature. A thermocouple provides temperature data, and a resonant laser beam passing through the tube produces fluorescence when the IHOPG begins to emit rubidium. Once we observe laser-induced fluorescence, we note the current temperature as the activation temperature and raise the temperature an additional 40 °C for 8 hours. The goal of this 8 hour period is to deplete the rubidium at the edges of the IHOPG, which we suspect reduces its availability to react with local atmosphere. Samples treated in this way have been handled in air for 90 minutes or more with no visible changes. Without this second step, the sample turns grey as a coating of rubidium hydroxide forms on the surface. Samples with this coating have still been used to load a MOT.¹⁸ However, these reactions are usually best avoided, as they may cause physical damage, making heating the IHOPG more difficult. For example, a crack could impair inductive heating, or disconnect the dispenser from its heater.

III. APPARATUS

In sections IV and V, we will discuss two comparisons between IHOPG dispensers and commercial rubidium chromate dispensers. This section describes the apparatus used to perform both of those comparisons. A schematic view of the chamber is pictured in Figure 1. On the left, a rectangular glass chamber provides optical access for a 3D MOT (red laser beams). The IHOPG and a chromate dispenser were located near each other, in the cylindrical glass neck between the glass and steel parts. A sputter-ion pump and a residual

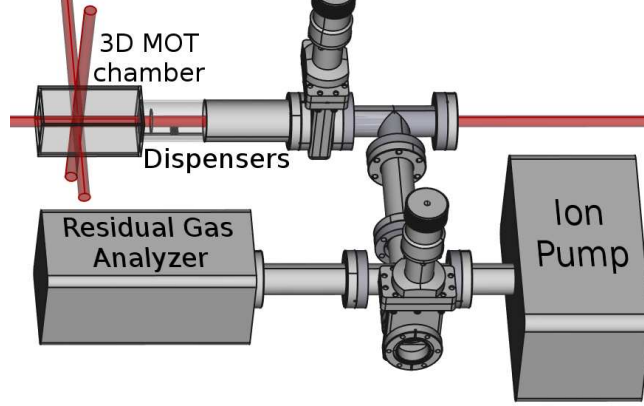


FIG. 1. The chamber used for the experiments in Sections IV and V. The two different dispensers rest near each other in the glass neck at the top of the figure. The rubidium fluorescence is measured at the crossing of the three beams, pictured in red. The retro-reflecting optics for the 3D MOT, the magnetic quadrupole coils, and the inductive heating coils are not shown.

gas analyzer (RGA) were attached to the steel part of the test chamber. The RGA measured partial pressures using a quadrupole mass analyzer, but measured the total pressure using a separate ion gauge filament. The unit used in these experiments was new, and for a measured total pressure of 1.3×10^{-8} Torr the sum of the pressure peaks from the mass spectrometer was 9×10^{-9} Torr. The RGA measured mass/charge ratios out to 90 AMU/e.

The two types of dispensers were oriented in perpendicular planes to permit selective inductive heating. The power transferred by an inductive heater is highly dependent on the spatial orientation of the coils and the object to be heated. The inductive heater coil for the chromate dispensers was wrapped around the cylindrical glass chamber and moved back and forth along the cylindrical section, changing its distance from the chromate dispenser to control its temperature. A different coil was placed under the IHOPG and moved up and down to control its temperature. The linear translation stages used to move the coils had 8 mm of travel. Due to space constraints, only one coil was in position at any given time. The two dispensers were only a few millimeters apart in the chamber, but based on the effective ranges of the inductive heaters (less than 8 mm), and on how strongly the orientation of the heaters affects the level of heating, we are confident that the heating of each individual dispenser did not significantly heat the other. The orientation and size of the coil for the chromate dispenser makes the induced fields over the volume of the IHOPG very small. Similarly, the coil for heating the IHOPG was several millimeters from the

chromate dispenser and was much smaller than the chromate dispenser, meaning that it was extremely unlikely to induce significant currents in the chromate dispenser. In addition, the different activation temperatures make it highly unlikely that the chromate dispensers would be anywhere near activation when the IHOPG was heated. When the chromate dispensers were heated, the heating of the glass in the area of the IHOPG was minimal. The lack of local heating is attributed to the use of Litz wire for the chromate heater coil, which helped reduce the resistivity of the coil at the high frequencies produced by the inductive heater.

The rectangular glass chamber admitted three perpendicular, circularly-polarized laser beams. These three primary beams all contained light 13 MHz red-detuned from the $5\ ^2S_{1/2}, F = 2$ to $5\ ^2P_{3/2}, F = 3$ line in ^{87}Rb . A repumping beam, tuned to the transition between the $5\ ^2S_{1/2}, F = 1$ and $5\ ^2P_{3/2}, F = 2$ resonance, was aligned with the beam going from right to left in Figure 1, and could be turned on and off independently of the primary beams. The three primary beams had a total power of approximately 13 mW, and each beam had a waist of about 7 mm. The repump beam had 1.8 mW of light in a similarly sized beam. Each beam was retro-reflected through a quarter wave plate to produce the light fields necessary for a 3D MOT. Magnetic coils outside the vacuum chamber produced the necessary quadrupole field at the intersection of the three beams. The MOT ensured that the laser was locked to the same frequency for each run, and gave an early indicator of rubidium vapor output.

The sputter-ion pump maintained the chamber pressure near 1.3×10^{-8} Torr. The chamber was baked out for 5 days at $125\ ^\circ\text{C}$ using a turbomolecular pump to minimize impurities, but the Viton gasket seal on the exit valve limited the overall quality of the vacuum. The RGA measured a partial pressure of water vapor of 1.3×10^{-9} Torr, with additional peaks of hydrogen (2.7×10^{-9} Torr) and nitrogen and carbon monoxide (1.1×10^{-9} Torr, at the same mass value). Other, smaller peaks were also present at several common mass numbers (e.g. carbon dioxide), but they did not significantly change upon heating of either dispenser. Neither dispenser, when heated, introduced new significant peaks to the RGA traces. Rubidium vapor was strongly attenuated by the chamber walls, never reaching the RGA in measurable concentrations. However, the dispensers were run for periods of several hours per day for several days before taking data, in order to align the laser beams and test and optimize the fluorescence measurements.

Before taking data, each dispenser was individually degassed over the course of several

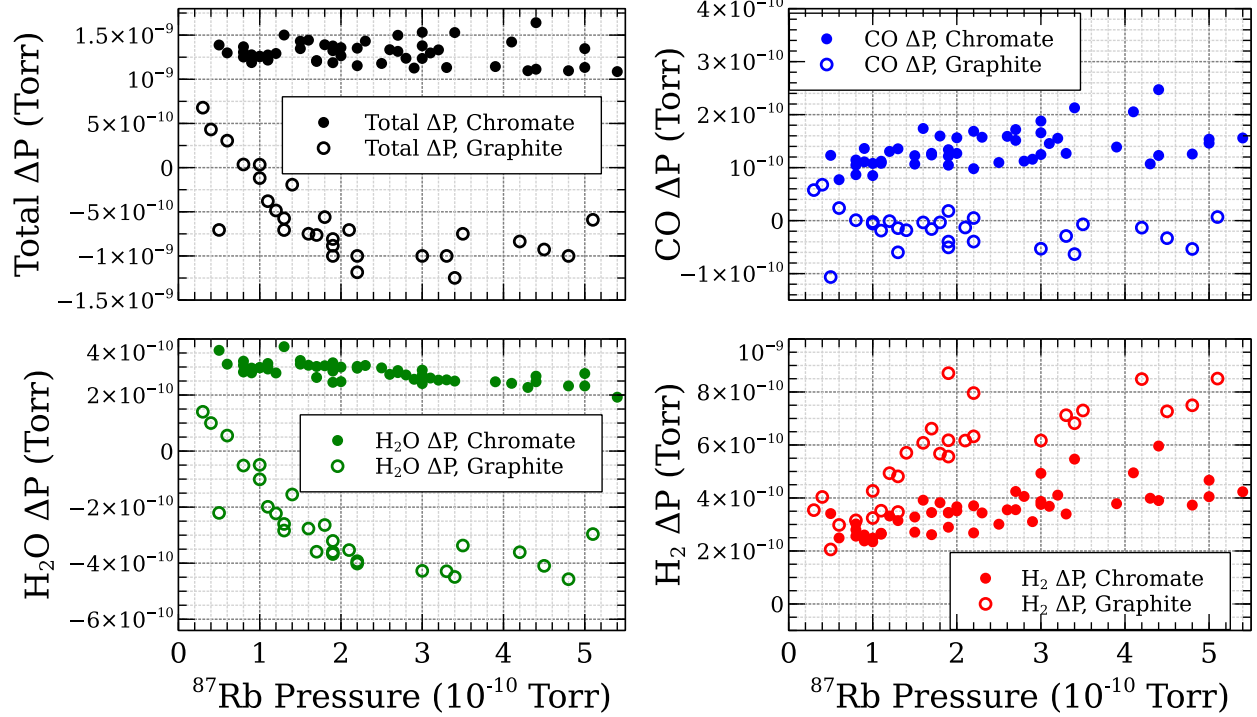


FIG. 2. Changes in total pressure and relevant partial pressures at steady-state with each dispenser type. The rubidium vapor density is approximated from fluorescence measurements. The vapor density is in turn determined by dispenser temperature and serves as an indicator of the emission rate.

hours. Each dispenser was slowly heated while the RGA monitored the released gases. The MOT beams provided feedback to determine when rubidium output began. As the temperature was increased, occasional bursts of output gas were measured on the RGA and were allowed to dissipate before further increasing the temperature. This process was continued until rubidium output was observed. The dispenser being used was then cooled to room temperature, and the background pressure in the chamber was allowed to stabilize, as measured on the RGA, before starting a run.

IV. STEADY-STATE OUTPUT COMPARISON

Each dispenser was heated individually to a steady-state to measure the output gases. With the small amounts of rubidium used, the steel chamber walls were never saturated with rubidium, so the rubidium vapor was not detected by the RGA. Instead, rubidium density

was measured by observing the fluorescence of the atoms illuminated by the MOT cooling beams, imaged onto a photodiode. The measurements used in Figures 2 and 4 were taken with the quadrupole field and repump light turned off, as day-to-day variations in MOT shape resulted in significant variation in measured MOT fluorescence. In contrast, the light from the untrapped atoms was much more repeatable from day to day, and the imaging system had a much clearer global maximum during alignment. Between the cylindrical neck where the dispensers were and the chamber where the fluorescence was measured, there was a glass plate with an aperture. Neither dispenser had direct line-of-sight access to the fluorescence chamber. Rather, each dispenser produced a local cloud of rubidium, and a fraction of the atoms were diffusely reflected by the walls into the fluorescence chamber. Since the steel half of the chamber effectively functioned as a pump for rubidium, the local rubidium density near the dispensers should be roughly proportional to the dispenser's emission rate. The mean free path in the system is expected to be much larger than the size of the system, so the atoms that are directed at the crossed laser beams should reach them relatively unimpeded.

Calculations assuming a room-temperature distribution of rubidium and using the measured powers and detunings of the beams provided a rough estimate of local rubidium pressure as a function of observed fluorescence. For each of the six laser beams, we calculated the total fluorescence F in photons per second:

$$F = n \int_{-\infty}^{\infty} d^3\vec{v} \int_{-0.0036}^{0.0036} d^3\vec{x} f(\vec{v}) \Gamma(\vec{x}, \vec{v}), \quad (1)$$

where \vec{x} and \vec{v} are position and velocity, respectively, n is the ^{87}Rb density, $f(\vec{v})$ is the 3D Maxwell-Boltzmann distribution

$$f(\vec{v}) = \left(\frac{m}{2\pi k_B T} \right)^{3/2} \exp(-m|v|^2/2k_B T), \quad (2)$$

and $\Gamma(\vec{x}, \vec{v})$ is the rate of spontaneous emission

$$\Gamma(\vec{x}, \vec{v}) = \frac{\gamma}{2} \frac{I(\vec{x})/I_{\text{sat}}}{1 + I(\vec{x})/I_{\text{sat}} + (2(\delta - \vec{k} \cdot \vec{v})/\gamma)^2}. \quad (3)$$

$I(\vec{x})$ is the intensity profile of the beam in question, assumed to be a Gaussian in two dimensions and constant in the third direction, as the beams were collimated. γ is the excited state linewidth ($2\pi \times 6.065 \times 10^6 \text{ s}^{-1}$), δ is the detuning ($-2\pi \times 13 \times 10^6 \text{ s}^{-1}$), \vec{k} is the beam's wave vector, m is the mass of ^{87}Rb , T is 300 K, I_{sat} is the saturation intensity (1.67 mW/cm^2),

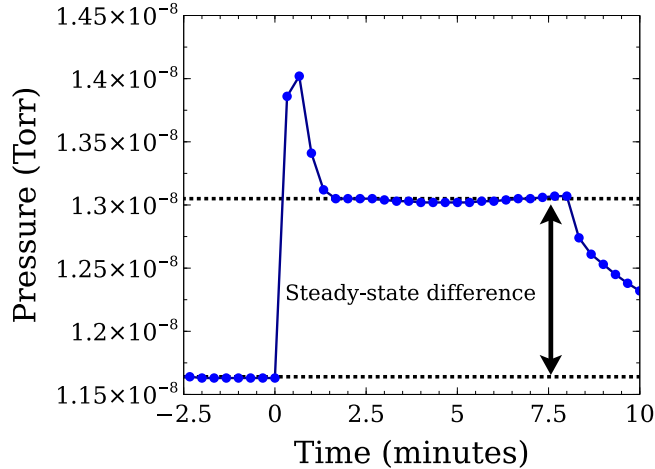


FIG. 3. An example of the RGA data used to produce one of the points in Figure 2. These data are from a run of the chromate dispenser, and correspond to total pressure measured by the RGA. When the dispenser is heated, the pressure spikes, then falls to an equilibrium pressure greater than measured before heating. The pressure difference between the measurement before turning on the dispenser and at steady state is plotted in Figure 2 against the rubidium fluorescence observed at steady-state.

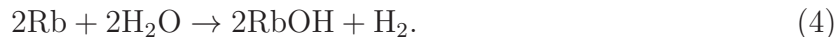
and k_B is Boltzmann's constant. The limits of the integral for position are determined by the field of view for the detector and its optics. The total number of photons was corrected for solid angle, efficiency of the detector, and amplification factor of the detector electronics. These calculations led to a rough estimate of the fluorescence emitted versus the number density (pressure) of the rubidium, corresponding to about 1×10^{-10} Torr of ^{87}Rb per millivolt of fluorescence. Since the six beams technically formed a three-dimensional molasses configuration, similar calculations estimated the additional contribution from slow atoms, assuming that all atoms with a velocity lower than 15 m/s were slowed to the recoil velocity, thereby increasing their time in the beams and emitted fluorescence. It should be noted that no effort was made to zero the magnetic fields, which will weaken the effect of the molasses. However, this overestimate leads to additional fluorescence from the slowed atoms that was less than that from the rest of the thermal distribution by about three orders of magnitude. The effect of the molasses is therefore negligible.

Figure 2 details the observed pressure changes as a function of rubidium output for the chromate and IHOPG dispensers. Each point represents a run in which one of the dispensers

was heated until the output gases measured by the RGA reached a steady state. In the case of the chromate dispenser, a typical run started with a large spike of output gases, followed by a taper over several minutes to reach a final plateau (see Figure 3). The chromate dispensers typically reached a steady-state after approximately ten minutes, and the IHOPG response times were somewhat slower. For low output rates, the IHOPGs acted in much the same way, but as the IHOPG temperature and rubidium output increased, a qualitative change in the IHOPG behavior occurred due to the background water vapor in the chamber.

During runs with the IHOPG at temperatures above a threshold corresponding to about 1 mV of rubidium fluorescence, the pressure curves measured by the RGA eventually fell below those measured before heating. In these cases, the pressure decrease continued very slowly over a fairly long period. The IHOPG data shown in Figure 2 were limited to 40 minutes of run time per point. The 40 minute duration was chosen to capture the majority of the effect while constraining experimental time. A few tests of the IHOPGs at longer times, up to two hours, showed that the 40 minute time limit captured the vast majority (> 90%) of the effect.

Comparing the total pressure to the water vapor pressure, it is clear that much of the pressure decrease is due to the rubidium vapor reacting with background water vapor:



The chamber used in this experiment had a significant background including water vapor. However, in a UHV chamber, the getter effect of the rubidium would not be present. The well-known characteristics of the RGA measurement make it possible to approximate the pressure change in a chamber without background water vapor. We take the total pressure data and add the lost water vapor back to each individual point. Figure 4 shows the data after this correction. Instead of simply adding back the lost water vapor, the data are corrected for the measured sensitivity differences between the mass filter and ion gauge filament, as well as for the measured ratio of the correlated 17 AMU/e peak. Correcting for the lost water vapor, the total pressure change is still well below that observed from the chromate dispenser over the measured range. As noted above, rubidium vapor was attenuated by the chamber walls before reaching the RGA. Therefore, the rubidium vapor pressure does not appear in the RGA total pressure levels.

The chromate dispensers did not produce a measurable decrease in water vapor despite

the emission of similar amounts of rubidium to the IHOPG dispenser. We attribute this to the fact that the activation temperature for the chromate dispenser is much higher, resulting in greater sympathetic heating of nearby chamber walls and desorption of water vapor from the walls. Even though the rubidium from the chromate dispenser was reacting with similar amounts of water vapor, the amount of water vapor released by heating the chamber walls exceeded the amount reacting with the rubidium. A careful examination of Figure 2 shows that the water vapor output when heating the chromate dispenser has a weak negative slope as the rubidium output increased. The amount of additional desorption as the dispenser temperature was raised was less than the getter effect of the additional rubidium, but the high activation temperature meant that there would be significant heating of the chamber even at very low rubidium output rates.

In a chamber without background water vapor, the pressure decrease shown in Figure 2 would likely not appear, but the corrected data in Figure 4 suggest that the pressure increase due to undesired gas emission from the IHOPG is extremely small. In comparison, the chromate dispensers increased total background pressure by about 1.2×10^{-9} Torr regardless of the level of rubidium output. In the worst case, when the IHOPG was producing almost no rubidium, the total pressure increase in the steady state was 7×10^{-10} Torr. These results show that in the configuration used here, the IHOPGs produce, at most, about one-half of the waste gases of the chromate dispensers, and compare more favorably at higher output rates. Some of the observed waste gases were almost certainly contributed by desorption of gases on nearby walls, but this effect is difficult to engineer away, as the heat required for activation, especially for the chromate dispensers, is quite large. In other words, there seems to be a significant advantage to be gained by using dispensers that require less heat to activate, as generating less heat mitigates desorption and out-gassing from other nearby vacuum components.

V. GAS ABSORPTION COMPARISON

UHV systems have extremely stringent requirements on their contents. Even extremely clean materials can outgas enough to have a measurable effect on vacuum quality. Background gases adhere to the surfaces of the chamber or diffuse through chamber materials, creating a persistent gas load. Heating the chamber or its contents, e.g. a dispenser, re-

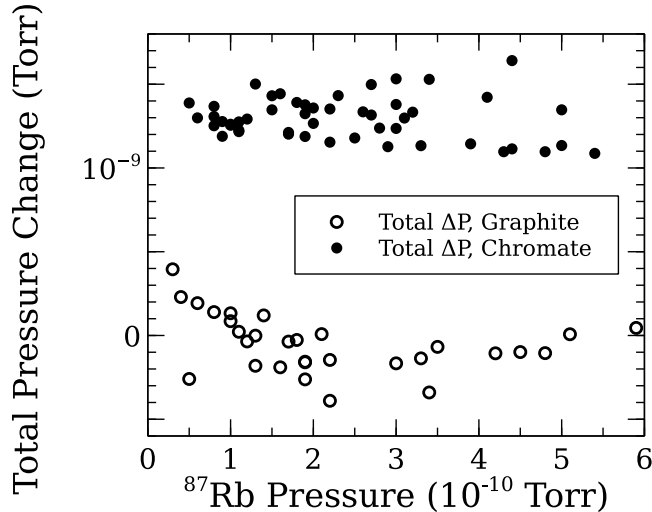


FIG. 4. Total pressure comparison, with the graphite dispenser data corrected for reactions between water vapor and rubidium. The chromate dispenser data are unchanged from Fig. 2, and are shown for reference only. The pressure loss due to dispensed rubidium reacting with background water vapor has been added back to the IHOPG data, using best estimates for the sensitivity differences between the mass spectrometer and ion filament, as well as the measured ratio of the 17 AMU peak to further refine the correction. These data provide approximate values for the expected pressure differences that would be observed in a chamber without background water vapor. Of note is that even with the water vapor losses added back to the IHOPG data, the total pressure increase is near zero, and still much less than the observed pressure increases from the chromate dispenser, even without correcting those data for the water vapor reaction.

leases even more gas. We have observed significant gas loads produced by commercial chromate dispensers when heating them, especially after leaving them at room temperature for extended periods. For example, in one chamber, a SAES NEXTorr D 100-5 sputter ion/non-evaporable getter (NEG) hybrid pump normally runs currents at the lower limit of observation, between 0 and 1 nA, corresponding to pressure at or below 1.5×10^{-11} Torr. After 72 hours with the dispenser at room temperature, heating the chromate dispenser significantly increases the ion pump current. The increase depends on how rapidly the dispenser is heated, but currents of 5-6 nA ($7.7 - 9.2 \times 10^{-11}$ Torr) during the first hour of heating are common. Longer periods of inactivity seem to result in larger currents. Whether this is caused by adsorption of waste gases onto the steel portion of the dispenser or reversible absorption into the getter material is not certain, but it is reasonable to suppose that a

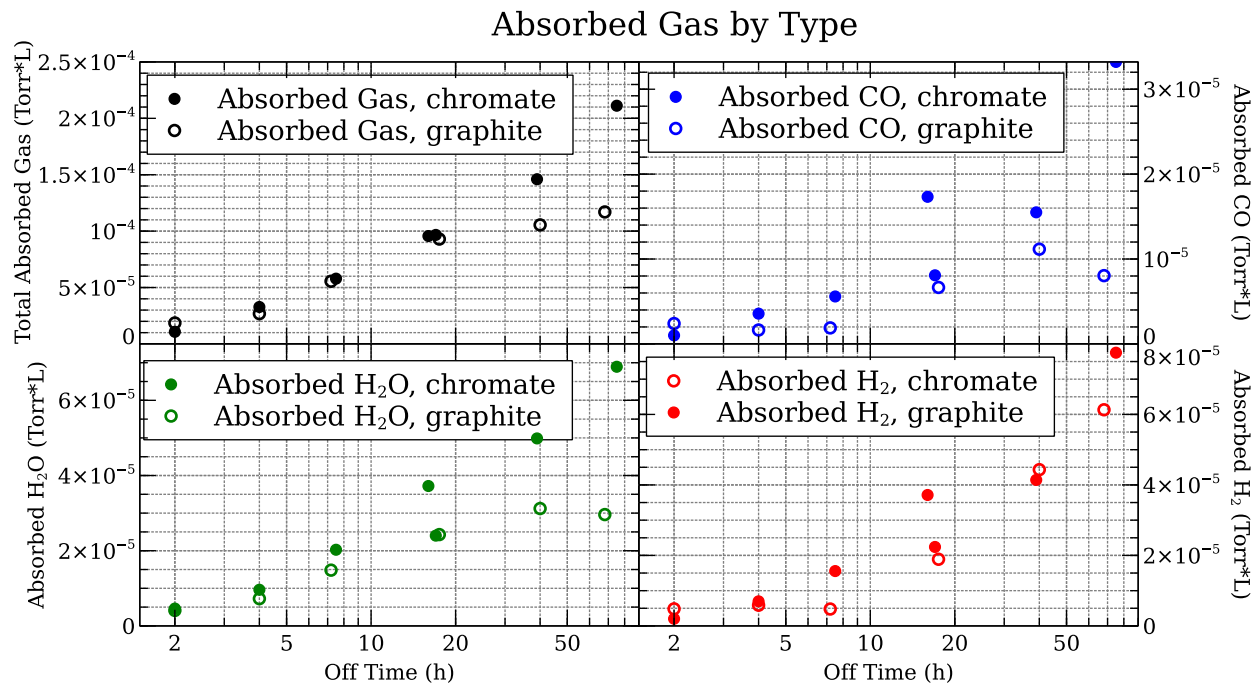


FIG. 5. Measurements of absorbed gas in the different dispensers or adsorbed to nearby surfaces heated along with the dispenser. Each point is derived by integrating the area under a difference curve calculated by subtracting the pressure curve of a one-hour off-time from the chosen, longer off-time, and then multiplying by the pumping rate. See Figure 6 for a set of example data.

dispenser without dedicated internal getter material might collect less gas over time. The experiment described below tests this hypothesis, comparing adsorbed/absorbed gases from IHOPG and chromate dispensers after various periods left at room temperature.

In order to measure absorbed gas, the dispensers were left at room temperature for a range of times between 2 and 72 hours, and then heated to a constant temperature, corresponding to about 1.8 mV of fluorescence, or about 2×10^{-10} Torr of ^{87}Rb in the glass chamber. During the heating process, the RGA measured various gas pressures every few seconds. The resulting curves were compared to a curve produced by the dispenser after 1 hour at room temperature (i.e., when almost no gas should have been absorbed). The area difference between the curves is proportional to the total waste gas released, as illustrated in Figure 6. The total gas released is approximated by multiplying the area between the curves by the pump rate of the ion pump. Figure 5 shows the results of these tests and calculations.

The results show that both dispensers and the sympathetically-heated parts of the chamber collect similar amounts of gas up to about 24 hours at room temperature. At longer

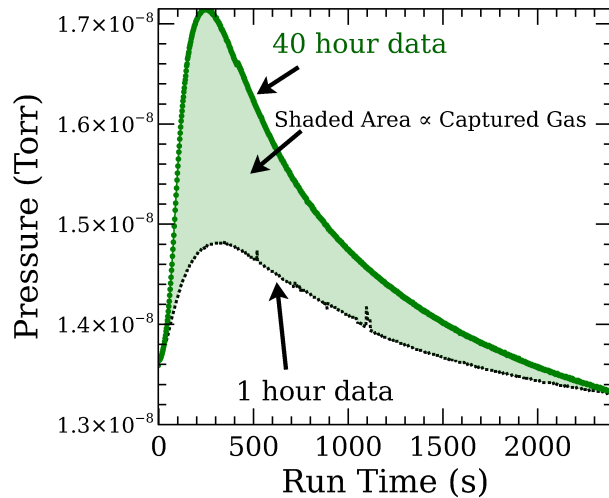


FIG. 6. Example of pressure data used to produce the 40 hour point for IHOPG gas absorption measurement. The lower curve shows the total pressure as a function of time when the IHOPG was heated after 1 hour at room temperature. The upper curve shows pressure data collected when the IHOPG was similarly heated after 40 hours at room temperature. The area difference between the two curves is used to determine the amount of gas absorbed by the dispenser during the 40 hour period. Each point in Figure 5 comes from one such comparison.

times, the chromate dispenser and the chamber around it continue to absorb, but the IHOPG levels off, except for hydrogen. This is unsurprising because rubidium intercalated graphite is known to act as a getter for hydrogen at room temperature.²⁴ These results suggest that the IHOPG dispensers attract less total waste gas than the chromate dispensers when left cold for an extended period, though the amount of the effect which can be attributed to the dispenser rather than nearby chamber walls is difficult to determine. However, the data suggest that the IHOPG may have additional utility in experiments where long (days or longer) periods of inactivity are expected, in addition to their overall lower level of undesired gas output.

VI. CONCLUSIONS AND OUTLOOK

Experimental data and observations show that IHOPG is a suitable source for clean rubidium vapor in a cold atom experiment. IHOPGs consist of relatively inexpensive and easily available materials, and their production requires equipment typically available to atomic

physics laboratories. They are operated with similar equipment to chromate dispensers, but require less power to operate and produce much less waste gas. Handling time in air can be increased to over 90 minutes with simple post-processing. Under most circumstances, this should be enough time to mount the IHOPG and bring the chamber down to rough vacuum. Another potential issue with IHOPGs is the low maximum baking temperature, which is limited to the activation temperature of the IHOPG, between 125 and 150 °C, but these temperatures are often enough to bake out a chamber, albeit over a longer period. Since the expected temperatures needed to intercalate lithium and potassium are higher, it is possible that IHOPG dispensers using those metals will have higher activation temperatures, which would require more power to dispense gas but allow higher maximum bake out temperatures.

The increased capacity per mass and volume of IHOPGs is an advantage in experiments where long-term operation without service is necessary, such as space applications. The high purity of the output vapor reduces load on the vacuum pumps, and minimizes the increase in background pressure, which may be especially useful in experiments requiring a compact form factor, where, for instance, differential pumping schemes might not be feasible.

Since cesium, potassium, and lithium are known to intercalate into HOPG with relative ease, they are excellent candidates for dispenser production as well. Cesium's applicable thermodynamic characteristics are very similar to that of rubidium, so loading and dispensing may work at very similar temperatures. Potassium and lithium have a much lower vapor pressure for a given temperature, so higher temperatures will almost certainly be required to load and activate the dispenser, but these temperatures may still be lower than those required for a potassium or lithium chromate dispenser.

The production of IHOPGs is simple and inexpensive. They can be produced with equipment readily available to most atomic physics labs. No highly technical skills are required to produce them. Therefore, they may find applications in undergraduate-level atomic physics experiments, where budgets are limited and students have not yet developed extensive technical skill.²⁵ As an undergraduate-level experiment, the production of IHOPGs could be used to instruct students on the use of a glove box, basic vacuum protocol, and safe handling of alkali metals.

IHOPGs have already been used in-house to load a 2D grating MOT. The atom numbers observed in the 2D and 3D grating MOTs were very favorable compared to other similar

experiments,^{18,26-28} despite using less overall laser power than other grating-based systems. An IHOPG is currently in use on an experimental apparatus that regularly produces Bose-Einstein condensates. The vacuum chamber was changed over from one with a chromate dispenser to one with an IHOPG and has experienced a noticeable improvement in the lifetime of atoms in the magnetic trap, from around 2 seconds to 5 seconds. The lifetime in the IHOPG chamber has remained at this level after about 1 year of nearly continuous operation. This, in addition to the data described here, suggest that the integration of IHOPG dispensers into systems is practical and can improve their behavior, compared to chromate dispensers. Our experimental apparatus currently under construction are moving over to IHOPG from chromate dispensers whenever feasible.

VII. ACKNOWLEDGMENTS

This work was funded by the Air Force Research Laboratory. We wish to thank Dr. Greg Pitz and Joshua Key of AFRL for additional help in producing IHOPGs.

REFERENCES

- ¹Y. J. Lin, A. R. Perry, R. L. Compton, I. B. Spielman, and J. V. Porto, *Phys. Rev. A* **79**, 063631 (2009).
- ²M. R. Walkiewicz, P. J. Fox, and R. E. Scholten, *Rev. Sci. Instrum.* **71**, 3342 (2000).
- ³SAES Getters, “Alkali Metal Dispensers,”
https://www.saesgetters.com/sites/default/files/AMDBrochure_0.pdf (2007).
- ⁴Various commercial equipment, instruments, and materials, as well as their suppliers are identified in this paper to foster understanding and reproducibility. These identifications do not imply endorsement by the Air Force Research Laboratory, or that other materials are unsuited to these purposes.
- ⁵J. Fortagh, A. Grossmann, T. W. Hänsch, and C. Zimmermann, *J. Appl. Phys.* **84**, 6499 (1998).
- ⁶W. Rüdorff and H. Schulz, *Z. Anorg. Allg. Chem.* **245**, 121 (1940).
- ⁷R. C. Croft and R. G. Thomas, *Nature* **168**, 32 (1951).

- ⁸S. R. Jefferts, J. Shirley, T. E. Parker, T. P. Heavner, D. M. Meekhof, C. Nelson, F. Levi, G. Costanzo, A. De Marchi, R. Drullinger, L. Hollberg, W. D. Lee, and F. L. Walls, *Metrologia* **39**, 321 (2002).
- ⁹F. Levi, L. Lorini, D. Calonico, and A. Godone, *IEEE Trans. Instrum. Meas.* **52**, 267 (2003).
- ¹⁰J. A. Baumann, D. G. Brock, M. A. Kuck, and G. K. Miller, “Graphite intercalated alkali metal vapour sources,” European Patent 0130803A2 (1985).
- ¹¹D. Guerard and A. Herold, *Carbon* **13**, 337 (1975).
- ¹²Z. X. Shu, R. S. McMillan, and J. J. Murray, *J. Electrochem. Soc.* **140**, 922 (1993).
- ¹³B. Jungblut and E. Hoinkis, *Phys. Rev. B* **40**, 10810 (1989).
- ¹⁴F. J. Salzano and S. Aronson, *J. Chem. Phys.* **43**, 149 (1965).
- ¹⁵F. J. Salzano, *J. Chem. Phys.* **45**, 4551 (1966).
- ¹⁶S. Aronson, F. J. Salzano, and D. Bellafiore, *J. Chem. Phys.* **49**, 434 (1968).
- ¹⁷R. Asher, *J. Inorg.Nucl. Chem.* **10**, 238 (1959).
- ¹⁸E. Imhof, B. K. Stuhl, B. Kasch, B. Kroese, S. E. Olson, and M. B. Squires, *Phys. Rev. A* **96**, 033636 (2017).
- ¹⁹M. Ohler, M. del Rio, A. Tuffanelli, M. Gambaccini, A. Taibi, A. Fantini, and G. Pareschi, *J. Appl. Crystallogr.* **33**, 1023 (2000).
- ²⁰H. Bremer, F.J. and Bleichert, in *Concise Encyclopedia of Materials Characterization*, edited by E. Cahn, R.W. and Lifshitz (Pergamon Press, Inc., 1993) p. 165.
- ²¹L. Stout, G.H. and Jensen, *X-ray structure determination: a practical guide* (Macmillan, New York, 1968) p. 24.
- ²²F. J. Salzano and S. Aronson, *J. Chem. Phys.* **42**, 1323 (1965).
- ²³D. E. Nixon and G. S. Parry, *J. Phys. D: Appl. Phys.* **1**, 291 (1968).
- ²⁴K. Ichimura and M. Sano, *J. Vac. Sci. Technol., A* **10**, 543 (1992).
- ²⁵C. Wieman, G. Flowers, and S. Gilbert, *Am. J. Phys.* **63**, 317 (1995).
- ²⁶C. C. Nshii, M. Vangeleyn, J. P. Cotter, P. Griffin, E. A. Hinds, C. N. Ironside, P. See, A. G. Sinclair, E. Riis, and A. S. Arnold, *Nat. Nanotechnol.* **8**, 321 (2013).
- ²⁷M. Vangeleyn, P. F. Griffin, E. Riis, and A. S. Arnold, *Opt. Lett.* **35**, 3453 (2010).
- ²⁸J. Esteve, *Nat. Nanotechnol.* **8**, 317 (2013).